Computers & Operations Research 185 (2026) 107248

Contents lists available at ScienceDirect

Computers and Operations Research

journal homepage: www.elsevier.com/locate/cor

Optimal planning of power distribution networks with fault-tolerant configuration

Renato Bruni [a,*], Alberto Geri [b], Marco Maccioni [b], Ludovico Nati [b]

[a] Dip. di Ingegneria Informatica, Automatica e Gestionale, Università di Roma "Sapienza", Roma, 00185, Italy
[b] Dip. di Ingegneria Astronautica, Elettrica ed Energetica, Università di Roma "Sapienza", Roma, 00184, Italy

ARTICLE INFO

Dataset link: https://doi.org/10.17632/8dp2mmf6t9.1

Keywords:
Distribution networks
Constraint generation
Combinatorial optimization
Planning
Fault-tolerance

ABSTRACT

Power Distribution networks are essential infrastructures that should be designed by satisfying two conflicting requests: cost minimization and reliability. While traditional network planning aimed at radial configurations, which are more similar to the typical working configuration of a network but are not fault-tolerant, modern techniques seek for meshed configurations, since these architectures are more fault-tolerant. Due to the complexity of the problem and the large size of nowadays instances, most of the techniques used for planning are based on heuristic approaches. Thus, they are usually unable to guarantee optimality and not even able to provide an assessment of the distance from the optimal solution. In this work, we address the challenge of planning a fault tolerant network through an exact approach, by introducing innovative Mixed-Integer Linear Programming models designed for the planning of meshed distribution networks with loop-feeder or open-loop topology. Differently from other techniques, our approach simplifies the formulation by avoiding the need for fault scenarios, significantly reducing the computational burden of the optimization problem. The outcomes of our approach are the generation of optimal meshed network, which effectively balance cost and reliability of the electric distribution system. Comprehensive studies on realistic test instances show the advantages of the proposed formulations.

1. Introduction

Distribution Networks (DNs) are essential infrastructures for the delivery of electricity, and should be able to perform their task in an efficient and reliable manner, particularly as urbanization, electrification and energy demand increase. Electricity is provided by means of a number of *primary substations* (PSs), also called *source nodes* or *roots*, and must be supplied to a number of *secondary substations* (SSs), also called *demand nodes*. Traditionally, these networks have been designed as radial configurations, due to their simplicity in operation and protection schemes, and because the typical working configuration of the network is radial. This means that the structure of the network corresponds to a spanning forest rooted in the source nodes and connecting them to the demand nodes, as exemplified in Fig. 1 left.

However, in case of fault of a branch of the network, such a simple radial structure does not contain alternate paths to reach the demand nodes that were served by that branch, see Fig. 1 right where the faulted branch is (9,10) and the demand nodes 9 and 12 remain disconnected. Therefore, with the rising need for greater reliability and flexibility, meshed network topologies are becoming more prevalent, even in less urbanized environments. A meshed configuration contains also redundant arcs, forming cycles or paths between primary substations, that are left unused (electrically disconnected) in operation, to ensure radiality, as exemplified in Fig. 2 left. The unused arcs, drown with gray dashed lines, can be exploited to generate alternate paths to demand nodes in case of fault, see Fig. 2 right where nodes 9 and 12 can still be supplied.

In general, when a fault occurs in a meshed architecture, the network can be reconfigured by the Distribution System Operator (DSO) by simply operating on the switches that are present in each branch, in order to disconnect unavailable equipment and supply the demand nodes that remained unsupplied after the fault. Complete service restoration can be achieved in very short times by exploiting the redundancy provided by the meshes, without the need to wait for bulky emergency generators or equipment repair works. Thus, the advantages of a redundant/meshed topology are evident. Note that these redundant paths only need to reach the demand nodes. If a root remain isolated, no loads remain unenergized (e.g. fault of (10,11) would leave root 11 isolated even in the meshed topology of Fig. 2, but this causes no problems).

* Corresponding author.
E-mail address: bruni@diag.uniroma1.it (R. Bruni).

https://doi.org/10.1016/j.cor.2025.107248
Received 30 April 2025; Received in revised form 31 July 2025; Accepted 14 August 2025
Available online 29 August 2025

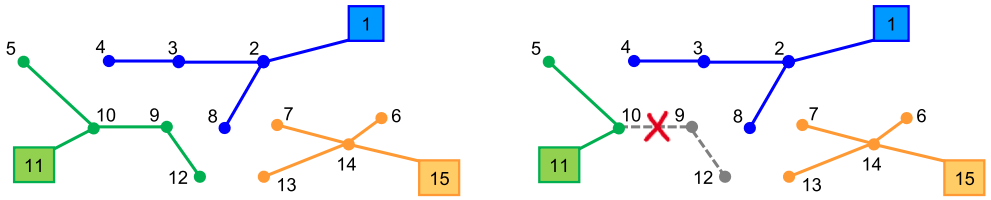

Fig. 1. Network with 3 root nodes (squares) and 12 demand nodes (dots) with simple radial topology and operating radially. In case of fault, some demand nodes are isolated.

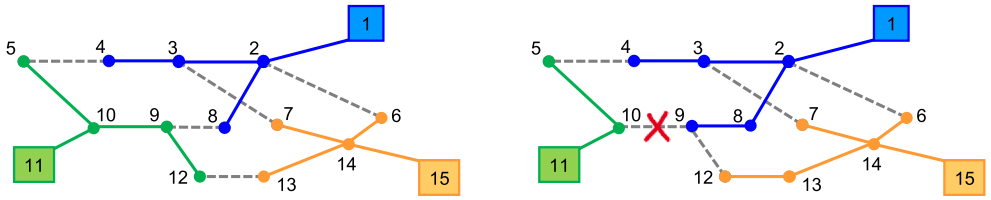

Fig. 2. Network with the same root and demand nodes, operating radially but having meshed topology. In case of fault, all the demand nodes can still be supplied.

1.1. Related works

Literature on electric power distribution network planning is quite vast, and the interest in the subject has dramatically increased in recent years (Rastgou, 2024). Broadly speaking, this research can be divided in two streams: one makes use of optimization and mathematical programming tools, the other relies on heuristics or meta-heuristics techniques.

Since the actual operation of the network is usually radial for a number of technical reasons, in the first stream many researches aim at incorporating radiality constraints directly in the optimization model used for planning. In particular, Lavorato et al. (2012) and Jabr (2013) introduce a methodological investigation on the formulations of radiality constraints making use of mathematical programming techniques. The same approach is further investigated in Wang et al. (2020), analyzing in better detail the issue of transfer nodes and pseudo-roots. Ref. (Muñoz-Delgado et al., 2018c) describes a multistage optimization problem from the perspective of a centralized planner, taking into account distributed generation. In this model, radiality constraints are used and thus the outcome is mostly a radial grid, apart from some meshes that might arise from connection of new loads in some stages.

Works (Asensio et al., 2018a,b) present a stochastic programming model directly considering the uncertainties of distributed energy resources and demand response.

Recently, Gust et al. (2024) propose a model for the design of distribution networks focused on the impact of demand coincidence called DNRP-LSDC. They find exact solutions for small instances, and develop solution heuristics for larger instances, given the NP-hardness of the considered problem. Therefore, in all the above works, meshes are not explicitly requested in the optimization models.

Ref. Muñoz-Delgado et al. (2018a) proposes a distribution network expansion planning model making use of the reliability indices shown in Muñoz-Delgado et al. (2018b). A similar approach is pursued by Jooshaki et al. (2022), using the metrics proposed in Jooshaki et al. (2020). In both cases, they assume that, on radial operation, the loads downstream of the faulted elements must wait for equipment repair to restore service, whereas the upstream nodes can be supplied after the faulted element is isolated. Anyway, both Muñoz-Delgado et al. (2018b) and Jooshaki et al. (2020) explicitly disregard post-fault network reconfiguration because they claim that it would render the problem computationally cumbersome and consequently the proposed models do not directly take into account meshes.

On the other hand, Li et al. (2021) proposes a distribution network planning model using the reliability indices described in Li et al. (2020). In these works, post fault network reconfiguration is incorporated in the optimization problem for a predefined set of equipment outage scenarios. Consequently, meshes are now obtained as a result of the proposed optimization problem. The same logic is applied in Wang et al. (2023), considering also other practical requirements of network operators, such as street layout constraints. The approach used in these works for ensuring redundancies and meshes, although correct from the mathematical point of view, suffers from heavy computational burden if applied to a large network with a significant number of outage scenarios, as pointed out in Muñoz-Delgado et al. (2018b) and Jooshaki et al. (2020). Going further in the direction of a meshed architecture, works (Bosisio et al., 2015, 2017, 2020) present an optimization model to plan a network with an H-shaped layout. Although this configuration is meshed and resilient to single fault, the model only works with an a-priori fixed number of feeders (4), each from a pre-selected PS. Thus the model is not expandable to a different number of roots, as admittedly reported in Bosisio et al. (2015).

Mathematical programming formulations have also been used for several other problems related to network design. For instance, Avella et al. (2005) seek to identify an optimal radial configuration to be used in operation in a meshed network, by viewing the feeder reconfiguration problem as a Steiner arborescence problem and using a mixed-integer quadratic programming solver. In the case of power distribution network reconfiguration, a recent work proposing a combinatorial optimization approach based on constraint generation is Nati et al. (2025). See also Crainic et al. (2021) for further examples.

The second research stream addresses the challenge of network planning through heuristics and meta-heuristics, that is, techniques not aiming at the optimal solution but at a (hopefully good) feasible solution.

In Díaz-Dorado et al. (2002) an evolutionary algorithm is presented to compute loop-feeder circuits topology; this configuration is meshed and reliable to single fault scenario. In Levitin et al. (1995) a genetic algorithm is used to plan a distribution network with open-loop topology, which is another meshed configuration resistant to single fault scenarios.

An iterative heuristic algorithm for the minimum cost open-loop network configuration is presented in Glamocanin and Filipovic (1993): after finding an initial open-loop configuration based on a set of heuristic rules, an iterative procedure based on power losses optimization is performed to improve the solution. In Gouin et al. (2015, 2017) a three stages heuristic is developed to optimize master plans of a distribution network, taking into account street layouts as well. The obtained

configuration is again an open-loop topology, called secured feeder architecture. Finally, a local search heuristic has been used in García and França (2008) for the similar problem of service restoration, consisting in performing a network reconfiguration for transferring unsupplied customers to energized support feeders.

1.2. Content of this work

In this work, we address the challenge to plan a meshed distribution network, with *loop-feeder* configuration or with *open-loop* configuration, through an exact approach, which currently appears to be an important research gap. Unlike previous works relying on fault scenarios to ensure redundancies, which Muñoz-Delgado et al. (2018b) and Jooshaki et al. (2020) suggest would make the model computationally cumbersome, our models do not require such scenarios. Moreover, the proposed models do not impose an a-priori number of feeders in the network, nor preselect the roots supplying the feeders. In contrast, these decisions are provided by the results of the optimization model.

We present three different Mixed-Integer Linear Programming (MILP) formulations, partially derived from Traveling Salesman Formulations however specialized to our problem. Two of them have an exponential number of constraints, and in these cases we present for both efficient separation procedures, in order to support a separation-optimization strategy, which is known to be more effective on large scale instances.

Since the formulation proposed for the open-loop case is by far the most computationally demanding among ours, we also try to improve it by adding some cut-based constraints. In summary, the contributions of this work can be listed as follows:

- Three different MILP formulations are presented to plan a meshed distribution network, with loop-feeders or open-loop topology, without the need to include in the model post-fault reconfiguration.
- For the two formulations that have an exponential number of constraints, we provide efficient separation procedures to find a violated constraint at integer nodes of the branch and cut process.
- We also identify some cut-based inequalities that can be added to the open-loop formulation to slightly modify the performance.
- We test the formulations and show the effectiveness on medium to very large scale instances.

The rest of the work is organized as follows: Section 2 formally describes the problem; Section 3 presents the proposed optimization models; Section 4 describes the separation procedures used to implement the proposed constraint generation framework; Section 5 provides computational results and discussion; Section 6 draws conclusions. The rationale of the cut-based constraints added to the open-loop formulation is in Appendix.

2. Problem description

We consider the problem of the distribution network planner seeking to build an entire new grid. This case arises in several situations, for example, in newly electrified environments, or when new voltage levels must be implemented, or in the complete renovation of an old infrastructure. It may also arise as a subproblem in the partial renovation of a larger infrastructure.

At the very basic level, there are a number of Primary Substations (PSs) and Secondary Substations (SSs) located in a territory, and the problem consists in selecting which of the possible connections must be built so that cost is minimized while (1) the service of each SS is ensured, and (2) a chosen degree of fault-tolerance is guaranteed. As in Gouin et al. (2017), we assume that the location of each PS and SS is already defined, and for each SS a reference load is given. We do not impose a-priori a limited set of candidate connections, thus in theory any substation of the network could be connected to any other. Moreover, as it is common practice between Distribution System

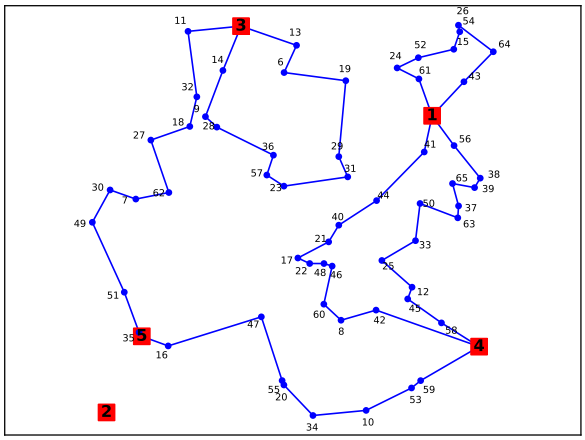

Fig. 3. Network with 60 SSs (blue dots) and 5 PSs (red squares) in loop-feeder topology.

Operators, we assume the use of a standardized power capacity for each electrical cable in the network, largely overscaled with respect to individual loads. The topology of the obtained network must be meshed, as better defined below, so that any single failure or maintenance work in the network can be solved through reconfiguration maneuvers without significantly impacting the quality of supply. Furthermore, we must ensure that in case of single fault, no overloads arise in the reconfigured network.

From the topological point of view, and regardless of the electric supply, a *power line* is a path in the network which starts from a PS, connects a certain number of SS and then ends on a PS. Different power lines cannot have SSs in common. Each branch of the network has switches at its extremities to interrupt the circuit when needed. This allows network reconfiguration. When the network is in normal operation, each SS must be electrically supplied by a single PS, i.e., the configuration must be *radial*. This means that, regardless of the underlying topological structure, the branches of the network supplying electricity take the shape of a spanning forest rooted in the PSs and connecting them to the SSs. Radiality in operation is obtained by opening one switch in each power line, splitting it in two parts: one part will be supplied by the PS at one end; the other part by the PS at the other end. The part of the power line supplied by a single PS is called a *feeder*.

The meshed topologies that we are interested in obtaining in this work are two known types: the so called *loop-feeder* topology and the so-called *open-loop* topology. The difference between the two is that loop-feeder topology may accept a power line with both extremes connected to the same PS, whereas open-loop topology requires that each power line has two different PSs at its extremes. To exemplify, Fig. 3 represents a network with loop-feeder topology, Fig. 4 a network with open-loop topology. Both networks contain several power lines, but only in loop-feeder topology the starting and the ending PS can be the same. In particular, Fig. 3 has two loops that close on the same PS, $\{3, 13, 6, 19, 29, 31, 31, 23, 57, 36, 28, 9, 14, 3\}$ and $\{1, 61, 24, 52, 15, 54, 26, 64, 43, 1\}$, while in Fig. 4 all power lines close on different PSs. Note that both topologies do not explicitly require that all PSs have at least one power line, as shown in Figs. 3 and 4 where PS 2 is not connected to any SS.

Thus, open-loop topology appears more demanding to obtain, as an open-loop network satisfies also the definition of loop-feeder, but not vice versa. Indeed, open-loop topology is more resilient than loop-feeder topology: both architectures guarantee the possibility to supply the SSs in case of any single branch fault, but loop-feeder architecture may fail in case of PS failures. This situation may occur in practice due to HV/MV transformer failure or more extreme conditions such as fire

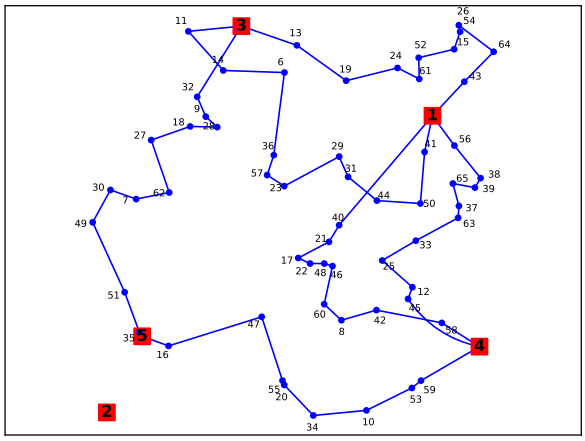

Fig. 4. Network with 60 SSs (blue dots) and 5 PSs (red squares) with open-loop topology.

Table 1
Summary of symbols for open loop network formulations.

Sets and indices	Description
N	Set of nodes
R	Set of roots, $R \subset N$
D	Set of demand nodes, $D \subset N$, $D = N \setminus R$
i, j, k	indices for the nodes
A	Set of arcs (branches)
(i, j)	indices of arcs viewed as ordered pairs of nodes, with $i < j$
Parameters	**Description**
d_i	Power demand of node i (in MW)
$p_{(i,j)}$	Power capacity of arc (i, j) (in MW)
$c_{(i,j)}$	Activation cost of arc (i, j)
Variables	**Description**
$x_{(i,j)}$	Activation of arc (i, j) (binary variables)
$f_{(i,j)}$	Power flowing through arc (i, j) (continuous). If positive the direction is from i to j, if negative from j to i
$s_{(i,j)}$	Fictitious power flowing through arc (i, j) (continuous). If positive the direction is from i to j, if negative from j to i.

or flood. In this scenario, the faulted PS and all its incident branches become unavailable. Thus, even after the post fault reconfiguration, all the SSs in the power lines having that PS at both extremes remain necessarily unsupplied. In contrast, open-loop topology guarantees the possibility of service for all the SSs even in this fault scenario. Note also that this need for reachability is limited to the set of SSs, while a PS can remain isolated without problems, since it does not need service.

Finally, we seek a grid architecture ensuring that, in the case of any single branch fault scenario, no overloads arise in the network. The most severe condition is a fault in the first or last branch of a power line (those connected to a PS), because in this case all the SS of the power line must be supplied by only one feeder, which is responsible for hosting all the load. This requirement is usually achieved by limiting the amount of loads in each power line directly in the design phase.

3. Mixed integer linear formulations

This Section describes the proposed formulations to find a network with loop-feeders or open-loop topology. We model the network with a directed graph $G(N, A)$ with set of nodes N and set of arcs A. The nodes represent PSs (roots) and SSs (loads). The set of roots is denoted as $R \subset N$; the set of loads, or demand nodes, is denoted as $D = N \setminus R$. Each demand node i has its demand d_i. Note that negative demand is allowed, so that the proposed models are flexible enough to support distributed energy sources. The arcs represent electrical connections that could be built or not, and are identified with the ordered couple of its extreme nodes (i, j). We model them as directed arcs to be able to consider the direction of flows, even if the connections in the real problem are physically undirected. To avoid the presence of couples of opposite arcs (i, j) and (j, i) representing the same physical connection, we only consider arcs (i, j) with indices $i < j$ (indices being integer numbers). Each arc (i, j) has an activation cost $c_{(i,j)}$, taking into account whatever is needed in practice to make the connection operative, and a maximum electric power capacity $p_{(i,j)}$.

To design the network, we need to identify the connections that should be built or activated. Thus, we use variables $x_{(i,j)} \in \{0, 1\}$ associated with arcs, with value 1 if arc (i, j) is used in the solution, and 0 otherwise.

To guarantee meeting the demands of the nodes and respect the capacities of the arcs, we need continuous power flow variables $f_{(i,j)} \in \mathbb{R}$ associated with arcs. Moreover, in the case of our first model, we use additional continuous variables $s_{(i,j)} \in \mathbb{R}$ associated with arcs, representing the flow of a fictitious commodity. Both types of flow variables are positive when the flow goes from i to j (in the direction of the arc), and negative otherwise. The complete list of elements used is reported in Table 1. To simplify the notation, the above variables will also be written as x_{ij}, f_{ij}, s_{ij}. Note that all the above variables only exist for $i < j$.

Our formulations are based on the basic requirement that each demand node must have two incident active arcs. In what follows, we denote by $\delta(k)$ the set of arcs having one end in node k, i.e. the star of k, while $\delta^+(k)$ will be its forward star and $\delta^-(k)$ its backward star. The objective is the minimization of the total cost of the activated arcs, which is a very basic aim. Note that the proposed models may support even more complex objective functions without invalidating the rest (constraints and solution strategy). Then, the connection of the network must be granted. This can be obtained with different mathematical techniques. A first option is by using the so-called Single Commodity Flow (SCF) constraints, where the mentioned fictitious commodity has to reach each node to guarantee that the solution obtained is connected. We obtain the following formulation, named **Loop-Feeder Single Commodity Flow** (LF-SCF).

$$\min \sum_{(i,j)\in A} c_{ij}\, x_{ij} \tag{1}$$

s.t.

$$\sum_{(i,j)\in\delta(k)} x_{ij} = 2 \qquad \forall k \in D \tag{2}$$

$$\sum_{(i,j)\in\delta^-(k)} f_{ij} = d_k + \sum_{(i,j)\in\delta^+(k)} f_{ij} \qquad \forall k \in D \tag{3}$$

$$\sum_{(i,j)\in\delta^-(k)} s_{ij} = 1 + \sum_{(i,j)\in\delta^+(k)} s_{ij} \qquad \forall k \in D \tag{4}$$

$$-(x_{ij}p_{ij})/2 \le f_{ij} \le (x_{ij}p_{ij})/2 \qquad \forall (i,j) \in A \tag{5}$$

$$-(x_{ij}|D|)/2 \le s_{ij} \le (x_{ij}|D|)/2 \qquad \forall (i,j) \in A \tag{6}$$

$$x_{ij} \in \{0,1\} \qquad \forall (i,j) \in A$$

In more detail, constraints (2) guarantee that each demand node has two incident activated arcs. Constraints (3) impose that the total electric power entering the generic node k equals its demand plus the total power exiting k, so guaranteeing flow conservation and demand satisfaction. Constraints (4) do something similar for the flow of the fictitious commodity, which must reach each node, as explained above.

Note that the electric flow appears in the model only to guarantee that the network configuration will be able to meet the demands and respect the capacities in case of failure of one branch. Therefore, there is no need for it to appear in the objective function. Constraints (5) impose that the flow must be in module not greater than half of the capacity (and not the full capacity) if the arc is active, whereas it must be 0 if the arc is not active. This comes from common practice (Gouin et al., 2017) to guarantee that, in case of fault of a single connection, the electric flow can be rerouted in the feeder without overloading (see

end of previous Section). In any case, our model may support even more complex techniques to guarantee reliability by simply changing these constraints (and not the rest). Finally, constraints (6) define a similar logical condition for the fictitious commodity flow, allowing the flow through an arc only if it is active.

A second option to guarantee connection is by means of Subtour Elimination Constraints (SEC), where a subtour is an undirected cycle (i.e. a set or arcs forming a cycle regardless of the orientation of the arcs) that is disconnected from the rest of the solution. We denote by $A(S)$ the set of arcs with both extremes in the generic subset of nodes S. We obtain the following formulation, named **Loop-Feeder Subtour Elimination** (LF-SE).

$$\min \sum_{(i,j)\in A} c_{ij}\ x_{ij} \tag{7}$$

s.t.

$$\sum_{(i,j)\in\delta(k)} x_{ij} = 2 \qquad \forall k \in D \tag{8}$$

$$\sum_{(i,j)\in A(S)} x_{ij} \le |S| - 1 \qquad \forall S \subseteq D,\ |S| \ge 2 \tag{9}$$

$$\sum_{(i,j)\in\delta^-(k)} f_{ij} = d_k + \sum_{(i,j)\in\delta^+(k)} f_{ij} \qquad \forall k \in D \tag{10}$$

$$-(x_{ij}p_{ij})/2 \le f_{ij} \le (x_{ij}p_{ij})/2 \qquad \forall (i,j) \in A \tag{11}$$

$$x_{ij} \in \{0,1\} \qquad \forall (i,j) \in A$$

In more detail, constraints (9) impose that, for every possible subset S of demand nodes of cardinality at least 2, the number of active arcs with both extremes in S is not greater than $|S|-1$. This because $|S|$ arcs or more with both extremes in S would produce a subtour not supplied by roots, since each node has two incident arcs.

In the two above formulations, we allow even meshes containing a single root, connected to both sides of the power line. Therefore, we obtain a network with a loop-feeder topology. In case this configuration is not enough, and we want to obtain an open-loop topology, we can modify the second formulation by imposing subtour elimination constraints even for the sets of nodes containing a single root. We obtain the following formulation, named **Open-Loop Subtour Elimination** (OL-SE).

$$\min \sum_{(i,j)\in A} c_{ij}\ x_{ij} \tag{12}$$

s.t.

$$\sum_{(i,j)\in\delta(k)} x_{ij} = 2 \qquad \forall k \in D \tag{13}$$

$$\sum_{(i,j)\in A(S)} x_{ij} \le |S| - 1 \quad \forall S \subseteq N,\ |S| \ge 2,\ |S \cap R| \le 1 \tag{14}$$

$$\sum_{(i,j)\in\delta^-(k)} f_{ij} = d_k + \sum_{(i,j)\in\delta^+(k)} f_{ij} \qquad \forall k \in D \tag{15}$$

$$-(x_{ij}p_{ij})/2 \le f_{ij} \le (x_{ij}p_{ij})/2 \qquad \forall (i,j) \in A \tag{16}$$

$$x_{ij} \in \{0,1\} \qquad \forall (i,j) \in A$$

Now, constraints (14) impose that, for every possible subset S of nodes (either root or demand, but with no more than one root) of cardinality at least 2, the number of active arcs with both extremes in S is not greater than $|S|-1$. This means that such an S cannot contain a cycle, so its nodes must be supplied by two distinct roots. In conclusion, the effect of these constraints is that every node is connected to two different roots by two distinct paths, hence the obtained network has open-loop topology.

Our experiments indicate that this formulation for the open-loop case is by far the most computationally demanding among our formulations. Thus, we also consider a variant of it, obtained by adding cut-based constraints derived from the (13)–(14), see also Appendix. In particular, given a subset S such that $|S \cap R| = 1$, let $S' = S \cap D$ be the set of demand nodes in S and $T = N \setminus (S)$ be the set of nodes outside of S. Now, $\delta(S', r)$ is the cutset in the graph between S' and $\{r\}$, hence the set of arcs connecting r to the rest of S, and $\delta(S', T)$ is the cutset between S' and T, hence the set of arcs connecting S' to the nodes outside S. The new constraint has the following structure, as explained in detail in Appendix.

$$\sum_{e\in\delta(S',T)} x_e \ge \sum_{e\in\delta(S',r)} x_e$$

We add these constraints for every S containing all demand nodes and one root taken in every possible way. The newly obtained formulation is named **Open-Loop SubTour Elimination + Cut Constraints** (OL-SE+CC).

4. Separation procedure

Models (7)–(11) and (12)–(16) do not need fictitious flow variables, but on the other side they use the Subtour Elimination Constraints (SEC). The number of such constraints is very large, since the number of possible subsets S grows exponentially with the number of nodes in the network. Therefore, these models may become intractable with direct approaches due to memory limitations, even for medium-sized instances. To overcome this limitation, we propose the use of a separation-optimization technique, which does not initially write SEC in the model, but is able to dynamically add only the violated ones during the solution process. Such constraint generation is widely used in the field of combinatorial optimization, however it requires some effort to be carefully designed for the specific model, in order to be computationally convenient. In particular, the algorithm for the generation of the violated constraints, called *separation procedure*, has to be developed from case to case.

In this section, we introduce two correct and efficient separation procedures designed to effectively solve large-sized instances of the models (7)–(11) and (12)–(16). These procedures, sketched in Algorithm 1 and 2, are based on the identification of the subgraphs derived by each incumbent integer solution computed during the solution process to produce valid inequalities violated by that solution. These inequalities are added as cuts during the solution of the model by means of a branch-and-cut routine operated by a commercial solver, in addition to the standard cuts already generated by the solver and to possibly generated cuts corresponding to fractionary solutions. Note, however, that the emphasis of present work is in the solution of an important practical problem; the description of its complete formulation would be beyond its scope.

Algorithm 1 Separation for Subtour Elimination

```
Initialization: take the values x̄ from the incumbent solution and define the corresponding graph H(N, A(x̄))
Find connected components:
connComponents ← PartitionIntoConnComp(H)
for each component in connComponents do
    S ← component                          ▷ get the current component
    if |S ∩ R| = 0 then
        Compute newConstraint
        AddLazyConstraint(newConstraint)
    end if
end for
```

The separation procedure for model (7)–(11) starts by defining the **undirected** subgraph $H(N, A(\bar{x}))$ of $G(N, A)$ obtained from an incumbent solution $(\bar{x}, \bar{f})$, with $A(\bar{x}) = \{(i,j) \in A : \bar{x}_{ij} = 1\}$. In other words, H is the graph given by the arcs which are active in that solution. The separation works by finding the connected components of H, which can be done in linear time. After this, it checks whether there exists at least one connected component S containing no roots. In this case, S defines

a subtour, so we add the constraint banning it (see also e.g. Nemhauser and Wolsey (1999) and Wolsey (2020) for further details on separation optimization). After adding all such constraint violated by solution $(\bar{x}, \bar{f})$, the constraint generation procedure continues the exploration of the branch-and-bound tree until a new incumbent solution is obtained. The separation procedure is again invoked on the new solution, and so on, until a solution non-violating any SEC is obtained. Experimentally, the number of constraints that must be added with this technique is generally much smaller than the number of all possible SEC, and thus this technique becomes convenient.

The separation procedure for model (12)–(16) instead uses a new graph $H(N^*, A^*(\bar{x}))$, again obtained by an incumbent solution $(\bar{x}, \bar{f})$, however containing also a new additional node n^* set adjacent to all the roots, as follows:

$$N^* = N \cup n^*$$
$$A^*(\bar{x}) = \{(i,j) \in A : \bar{x}_{ij} = 1\} \cup \{(n^*, r) | r \in R\}.$$

Algorithm 2 Separation for Subtour and Closed Loop Elimination

1: **Initialization:** take the values $\bar{x}$ from the incumbent solution and define the corresponding graph $H(N^*, A^*(\bar{x}))$
2: **Find biconnected components:**
$biConnComponents \leftarrow$ PartitionIntobiConnComp(H)
3: **for** each $bicomponent$ in $biConnComponents$ **do**
4: $S \leftarrow bicomponent$ ▷ get the current biconnected component
5: **if** $|S \cap R| \leq 1$ and $n^* \notin S$ **then**
6: Compute $newConstraint$
7: AddLazyConstraint($newConstraint$)
8: **end if**
9: **end for**

Now, Algorithm 2 finds the biconnected components BCC of the graph $H(N^*, A^*(\bar{x}))$, with the biconnected components defined as the blocks of $H(N^*, A^*(\bar{x}))$. Recall that a biconnected component is a subgraph such that, if we remove in any possible way one generic node and all its incident arcs, the rest of the component remains connected. This can be done again in linear time thanks to Tarjan's algorithm (Tarjan, 1974). After this, the procedure checks whether any of the biconnected components, neglecting the ones having n^*, has a number of roots less than or equal to 1. In this case, we have found a violated constraint in (14) with $S = BCC$, since $H[BCC]$ is a cycle with at most one root node.

5. Experimental results

5.1. Case studies

Due to the lack of a well established test network benchmark in the field of distribution grid planning, we generate the following four networks. They have been assembled to represent realistic instances of the problem, **ranging from medium to very large**, as explained below.

- Case54: 4 PSs, 50 SSs and 1431 candidate arcs
- Case78: 3 PSs, 75 SSs and 3003 candidate arcs
- Case104: 4 PSs, 100 SSs and 5356 candidate arcs
- Case154: 4 PSs, 150 SSs and 11,781 candidate arcs

For each test network, we considered a certain number of nodes located in the city center, with a higher spatial density, and other nodes located in the suburbs, with a lower spatial density, as shown in Table 2.

The load demand for each SS is calculated using the absolute values generated by two different Gaussian probability distributions, one associated with the SSs located in the city center with a mean of 0.4 MW and a standard deviation of 0.2 MW, and the other with the SSs located in the suburbs with a mean of 0.2 MW and a standard deviation of 0.6 MW. The cost of the edges connecting each pair of nodes is $30000 \cdot (1 + c)$ €/km, where c is a random number uniformly distributed between 0 and 0.1. In each network, we simulate a natural obstacle that may be present in a real case, such as a river, using a piecewise linear function. Whenever an edge crosses the obstacle, the additional cost of 1,000,000 € is added to the connection, much greater than that associated with the Euclidean distance. From those weights associated with physical connections, a weighted graph is now obtained by taking as cost of the arc going from source node s to target node t the cost of the minimum-cost path starting from s and ending in t. Lastly, for a random number of node triplets in the network, the triangle inequality is *intentionally* violated, so that the sum of the costs of two connections is less than the cost of the third connection. As an example, the graph of Case54 network (the smallest), including all its 1431 candidate arcs, is shown in Fig. 5, where the color of the arcs represents the cost of the connection. The main data for all test networks are available in Maccioni et al. (2024).

Table 2
Case studies: location of nodes and spatial density.

Case study	PSs		SSs		Spatial density	
	Center (#)	Suburbs (#)	Center (#)	Suburbs (#)	Center (nodes/km^2)	Suburbs (nodes/km^2)
Case54	2	2	25	25	3	0.74
Case78	1	2	30	45	7.75	3.92
Case104	1	3	60	40	7.63	1.59
Case154	2	2	80	70	6.83	1.5

Table 3
Main results of meshed network planning obtained by the proposed formulations.

Case study	Formulation	Best value	Gap (%)	Time (s)	Root gap (%)
Case54	LF-SCF	2,215,776	0	57.4	3.848
	LF-SE	2,215,776	0	20.9	3.848
	OL-SE	2,965,399	0	3503.3	28.154
	OL-SE+CC	2,965,399	0	1628.2	28.096
Case78	LF-SCF	2,975,514	0	680.6	29.558
	LF-SE	2,975,514	0	278.1	29.558
	OL-SE	3,016,757	1.2	[a]	30.521
	OL-SE+CC	3,016,756	1.1	[a]	30.519
Case104	LF-SCF	2,455,816	5.1	[a]	13.185
	LF-SE	2,455,816	4.3	[a]	13.185
	OL-SE	2,691,143	12.4	[a]	20.777
	OL-SE+CC	2,793,875	15.8	[a]	23.658
Case154	LF-SCF	3,359,027	3.6	[a]	12.772
	LF-SE	3,359,027	4.2	[a]	12.772
	OL-SE	14,897,286	78.9	[a]	80.332
	OL-SE+CC	15,266,123	79.4	[a]	80.797

[a] Means terminated for timeout after 21 600 s.

5.2. Experiments

All models described in Section 3 have been implemented in Python and solved using Gurobi Optimizer 10.0.1. Table 3 reports the value of the best solution obtained by each formulation within the time limit of 21 600 s (6 h), the optimality gap corresponding to that solution, and the computation time. In case the solution process is stopped for timeout before completely closing the optimality gap, we report * for the time. In this case, the provided solution is at least feasible and the corresponding optimality gap is even possibly smaller than the reported one. Sample experiments indicate that, by allowing considerable more computation time, the reported solutions are sometimes optimal or near-optimal, however closing the gap by exploring all subproblems in the branching tree would require very long times.

The cost of the solutions does not increase proportionally with the number of nodes in the instance, even if the number of arcs composing

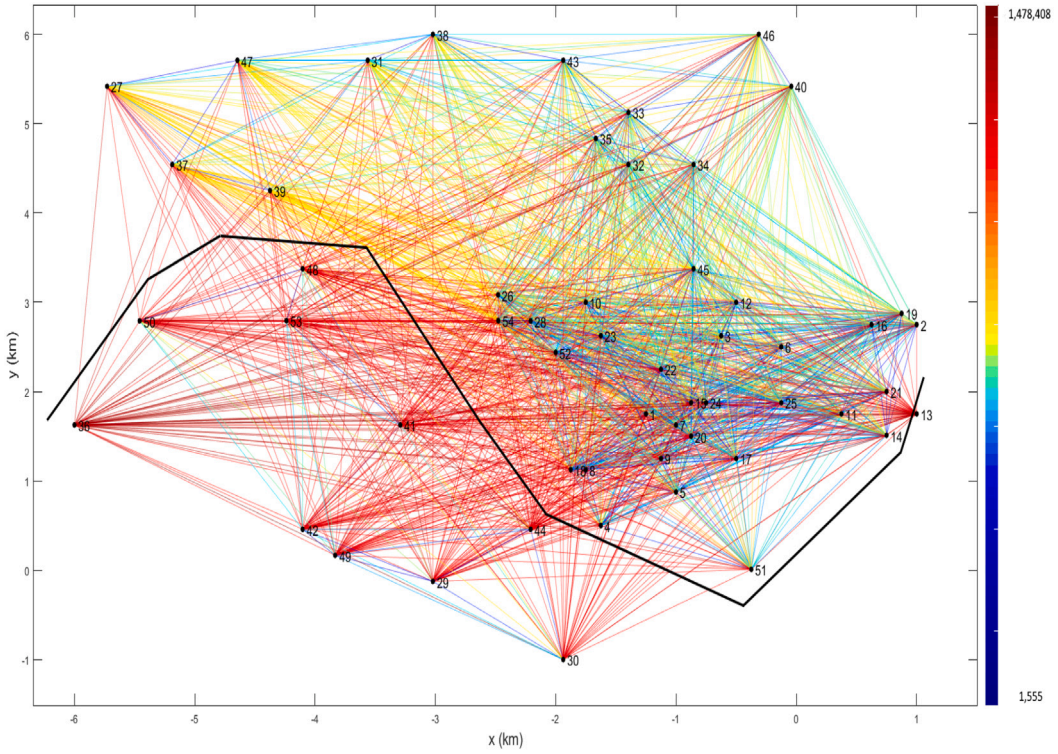

Fig. 5. Case54 test network: nodes are the black dots, the obstacle is the dark polygonal line. The color of each arc shows its cost, passing from lowest (blue) to highest costs (red).

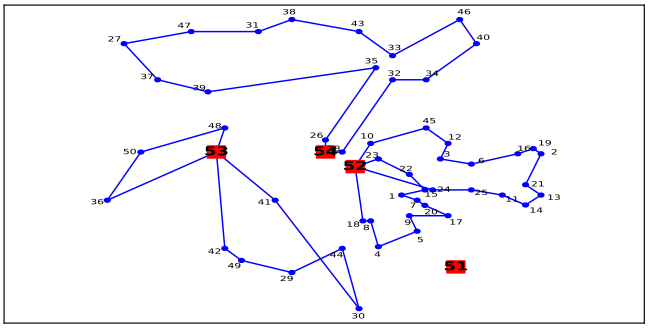

Fig. 6. Optimal topology of Case54 test network found by LF-SCF and LF-SE.

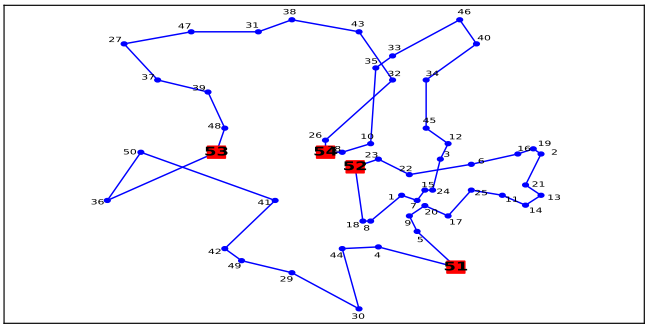

Fig. 7. Optimal topology of Case54 test network found by OL-SE and OL-SE+CC.

each solution obviously increases so. This holds because all the test networks have been generated by considering them insisting in an area of about 8 by 8 km, hence when the number of nodes increases,

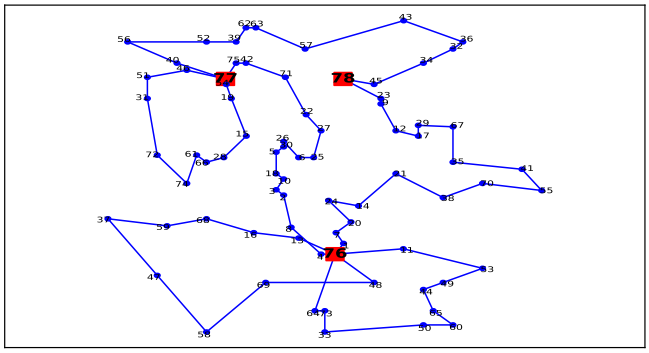

Fig. 8. Best topology of Case78 test network found by LF-SCF and LF-SE.

they simply become more dense and consequently the distances among nodes decrease. Since the cost of the arcs is initially roughly proportional to the distance, those costs decrease when increasing the number of nodes, and so the total cost of the solution does not go with the number of nodes. The list of candidate arcs selected by each formulation is provided in Maccioni et al. (2024).

Figs. 6 and 7, respectively, show the optimal loop-feeder and open-loop topologies of Case54 network, which is the only test network for which all the four formulations found the optimal solution within the time limit. For the other test networks, further experiments have been performed with reduced versions of the instances obtained by decreasing the number of candidate arcs. For each test network, we consider only the less expensive ten, three and one connections between any two nodes, respectively named LESS_10, LESS_3 and LESS_1 cases. In addition, connections between each SS and each PS have been included to ensure feasibility. These instances can represent several practical cases where the number of candidate arcs is less than every possible pair of nodes. Results are reported in Tables 4, 5, and 6 for

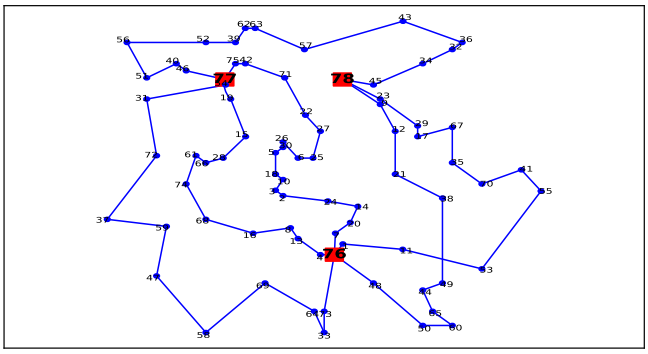

Fig. 9. Best topology of Case78 test network found by OL-SE+CC.

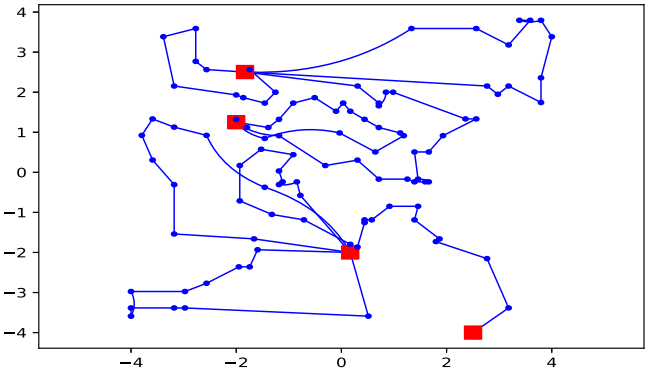

Fig. 10. Best topology of Case104 test network found by LF-SCF and LF-SE.

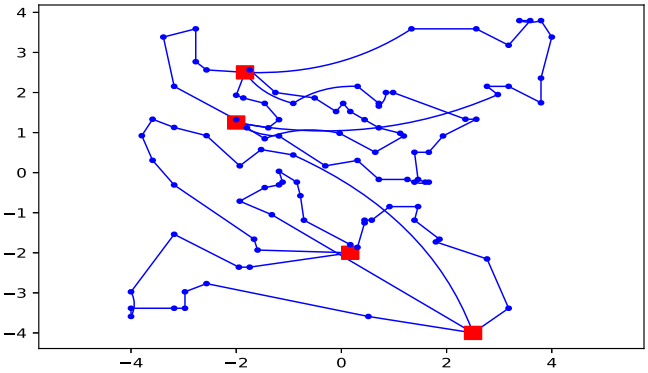

Fig. 11. Best topology of Case104 test network found by OL-SE.

Case78, Case104, and Case154 test networks, respectively. For these instances, we report the number of candidate arcs under the name of each case study. Note that LESS_1 cases represent a "greedy-style" filtering of the candidate arcs, which makes the feasible set much smaller, so the cost of the optimal solution tends to increase. The list of candidate arcs selected by each formulation is again provided in Maccioni et al. (2024), whereas Figures from 8 to 13 show the respective best loop-feeder and open-loop topologies.

5.3. Analysis of results

From the tables, we can observe that the first two formulations LF-SCF and LF-SE quite often produce the same solution at similar times, and are able to solve medium-sized instances to optimality and to find feasible solutions to large instances. They are even able to find the optimal solutions for the reduced versions of the largest instances.

Table 4
Results for Case78 test network with a lower number of candidate arcs, listed in parentheses for each case study.

Case study	Formulation	Best value	Gap (%)	Time (s)	Root gap (%)
Case78	LF-SCF	2,977,805	0	37.0	29.612
LESS_10	LF-SE	2,977,805	0	40.5	29.612
(846)	OL-SE	3,022,557	0.8	[a]	30.654
	OL-SE+CC	3,022,557	0.7	[a]	30.652
Case78	LF-SCF	3,105,404	0	24.2	32.049
LESS_3	LF-SE	3,105,404	0	22.9	32.049
(418)	OL-SE	3,160,284	0	83.2	33.229
	OL-SE+CC	3,160,284	0	31.3	33.227
Case78	LF-SCF	6,104,777	0	0.02	52.091
LESS_1	LF-SE	6,104,777	0	0.02	52.091
(291)	OL-SE	6,595,497	0	0.09	55.656
	OL-SE+CC	6,595,497	0	0.03	55.655

[a] Means terminated for timeout after 21 600 s.

Table 5
Results for Case104 test network with a lower number of candidate arcs, listed in parentheses for each case.

Case study	Formulation	Best value	Gap (%)	Time (s)	Root gap (%)
Case104	LF-SCF	2,466,677	3.1	[a]	13.253
LESS_10	LF-SE	2,464,502	3.0	[a]	13.177
(1255)	OL-SE	2,721,899	12.1	[a]	21.387
	OL-SE+CC	2,733,949	12.3	[a]	21.701
Case104	LF-SCF	2,548,815	0	385.5	15.279
LESS_3	LF-SE	2,548,815	0	142.6	15.279
(667)	OL-SE	2,774,754	3.1	[a]	22.178
	OL-SE+CC	2,774,754	3.6	[a]	22.146
Case104	LF-SCF	6,447,598	0	0.04	65.049
LESS_1	LF-SE	6,447,598	0	0.03	65.049
(497)	OL-SE	7,554,897	0	0.7	70.172
	OL-SE+CC	7,554,897	0	0.56	70.164

[a] Means terminated for timeout after 21 600 s.

Table 6
Results for Case154 test network with a lower number of candidate arcs, listed in parentheses for each case.

Case study	Formulation	Best value	Gap (%)	Time (s)	Root gap (%)
Case154	LF-SCF	3,381,413	2.0	[a]	12.740
LESS_10	LF-SE	3,380,337	2.5	[a]	12.712
(1937)	OL-SE	8,777,003	62.9	[a]	66.382
	OL-SE+CC	8,608,555	62.4	[a]	65.708
Case154	LF-SCF	3,614,274	0.9	[a]	18.371
LESS_3	LF-SE	3,614,274	0.8	[a]	18.371
(1006)	OL-SE	9,679,591	63.2	[a]	69.521
	OL-SE+CC	8,562,461	58.2	[a]	65.526
Case154	LF-SCF	9,316,662	0	0.08	67.418
LESS_1	LF-SE	9,316,662	0	0.05	67.418
(742)	OL-SE	28,818,305	0	7.1	89.466
	OL-SE+CC	28,818,305	0	7.99	89.461

[a] Means terminated for timeout after 21 600 s.

Hence, it appears that they can be used to determine loop-feeder networks in many practical situations. On the other hand, formulations OL-SE and OL-SE+CC are clearly more computationally demanding, however they are still able to determine at least feasible solutions even to the largest instances. This because the open-loop topology itself is more demanding to obtain, and its costs are much higher.

Since, as explained, no established benchmarks or codes are available in this field, comparing our results with the literature is not straightforward. However, to offer at least some insights for consideration, we can observe that for example Muñoz-Delgado et al. (2018a), with a MILP optimization approach to the multistage expansion planning problem (related but slightly different from our) solves an instance with 54 nodes and 63 branches in 47 min; Li et al. (2021) with another MILP optimization approach solves the reliability-constrained

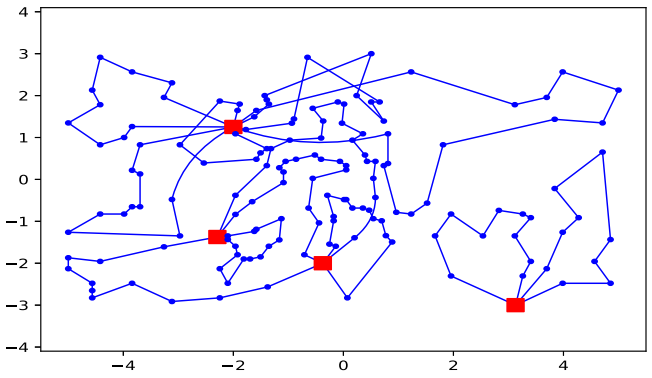

Fig. 12. Best topology of Case154 test network found by LF-SCF and LF-SE.

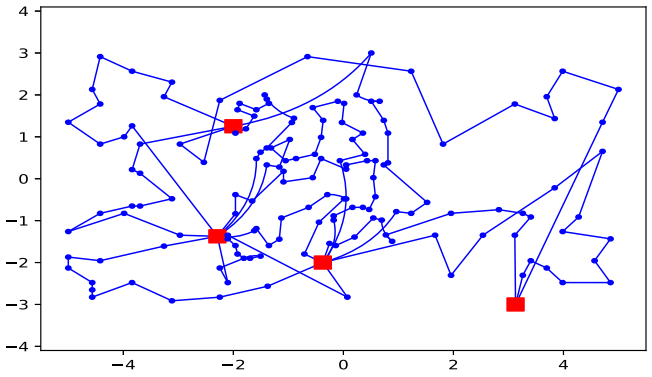

Fig. 13. Best topology of Case154 test network found by OL-SE+CC for LESS_3 version.

expansion planning problem (another variant) on the same instance in 50 min. Aslo Wang et al. (2023), using still another MILP optimization approach, solves the feeder planning problem (still another variant) with 36 nodes and 57 branches in 83 min. Our smaller problem has similar number of nodes (54) but a much larger number of branches (1431), and we solve it as in Table 3. The fact that our models can handle similar or larger problems in comparable times, even if for different versions of the planning task, contributes to confirm their effectiveness.

To give another evaluation of the quality the models, we compute, for every instance, the root node gap, defined as the (absolute) difference between the best found integer solution and the LP relaxation value at the root node of the branching tree, normalized by the best integer. This value provides a normalized metric, showing how tight the model is at the start.

The effectiveness of OL-SE+CC model, obtained from OL-SE by including additional cut-based constraints, appears unstable in the previous experiments. In particular, for the larger instances Case104 and Case154, the values of Gap and LP Gap are larger than those of the original OL-SE model. To better investigate this behavior, we consider the following Table 7, focusing on our constraint generation, node exploration, and root relaxation quality. We can observe what follows.

- The OL-SE+CC model indeed produces a stronger root relaxation, as expected, due to the presence of additional valid inequalities added at the beginning of the optimization.
- OL-SE+CC triggers fewer lazy constraints during the solution process than OL-SE. The presence of many explicit cut-based constraints early on may reduce the number of violated constraints detected during the branch-and-bound search.

Table 7
Solver statistics at the root node for OL-SE and OL-SE+CC.

Case study	Formulation	Root relaxation	Node count	N. Lazy cons
Case54	OL-SE	2,130,522.5	773,537	348
	OL-SE+CC	2,132,253.4	1,233,071	328
Case78	OL-SE	2,096,016.1	1,346,965	448
	OL-SE+CC	2,096,075.9	1,458,519	222
Case104	OL-SE	2,132,015.4	822,477	738
	OL-SE+CC	2,132,901.7	779,002	650
Case154	OL-SE	2,930,021.9	58,319	2427
	OL-SE+CC	2,931,545.0	78,557	1314

- Despite the stronger LP relaxation, OL-SE+CC often explores more nodes than OL-SE in the same time. Hence, it appears that the greater number of added lazy constraints in OL-SE might cause a larger overhead in solving the nodes when going deep in the branching tree, while OL-SE+CC node processing time remains more stable.

These findings suggest that OL-SE+CC and OL-SE models have different strengths and trade-offs. Although OL-SE+CC tightens the formulation early on, it can interact negatively with the constraint generation strategy, leading to a less effective search in some cases. Conversely, OL-SE benefits from a more dynamic constraint addition process, which may be more effective in guiding the solver in certain instances, however at a cost of a larger overhead in the solution of the deep nodes of the branching tree.

5.4. Limitations of this work and future research

The models proposed in this work are designed to plan distribution networks with fault-tolerant topologies without explicitly simulating post-fault scenarios. This choice significantly reduces computational burden and enables the use of exact methods on medium to large-scale instances. However, it also introduces some limitations.

The formulations assume that structural redundancy, achieved through loop-feeder or open-loop configurations, is sufficient to ensure service continuity under single branch faults. While this assumption is realistic in many practical settings, it does not account for the specific location, frequency, or type of faults that may occur in a real-world network. In particular, failures affecting multiple substations or other components simultaneously are not modeled.

We do not explicitly incorporate advanced fault localization or detection mechanisms into the planning phase. Recent works such as Ts-GSAN (Hu et al., 2025) and spectral-based event detection methods (Ma et al., 2021) offer powerful tools to identify and classify faults in real time. These methods, although operational in nature, could inform long-term planning by highlighting areas of greater vulnerability or likelihood of failure. Integrating such data-driven insights could enable more targeted reinforcement and risk-aware design strategies.

While our approach supports general topologies without predefining the number of feeders or their roots, it currently assumes homogeneous cable capacities and does not model power flow losses or voltage profiles. These assumptions simplify the optimization problem but may limit applicability in highly constrained or heterogeneous systems.

Moreover, this work focuses on a deterministic, single-period planning framework. Future research can extend the proposed MILP formulations to multi-period settings by replicating the decision variables across time steps and introducing inter-temporal constraints, such as investment budgets or asset lifespans. Similarly, stochastic extensions are possible using a scenario-based approach to model uncertainty in load profiles, distributed energy source generation, or weather-driven faults. These generalizations could be addressed through decomposition techniques. However, even in its current form, the model remains

applicable to realistic planning tasks when input parameters (e.g., demand or supply at nodes) are conservatively chosen based on design specifications or worst-case operating conditions. This is consistent with common engineering practice, where networks are dimensioned to handle peak or critical scenarios to ensure reliability and resilience.

Furthermore, the proposed models do not consider any preexisting network in place. Future research may extend the proposed approach to encompass network expansion. Lastly, another possible extension is the definition of tailored separation procedures implementing cut management strategies at fractional solutions.

6. Conclusions

Planning power distribution networks with a fault-tolerant configuration, in particular loop-feeder or open-loop topology, is a computationally demanding task, even because the size of real-life problems constantly tends to increase. In this work, we have presented mathematical programming formulations to solve this problem. For the two formulations that have an exponential number of constraints, we have also presented efficient separation procedures allowing to solve large-sized realistic instances in reasonable times, which are made publicly available (Maccioni et al., 2024). Even when the solution of our branch-and-cut procedure is not proved to be optimal, because the solution is terminated for time-out and the optimality gap is not completely closed, the obtained networks have useful features. Therefore, the proposed formulations can be used for the planning of fault-tolerant power distribution networks in many practical situations. Our experiments confirm that producing a network with open-loop topology is a more challenging problem than obtaining loop-feeder topology, particularly as the size increases. Future work will include the introduction in our models of the voltages in the SS, the generation of cuts corresponding to fractionary solutions to solve the open-loop formulations, the use of heuristic techniques to find starting feasible solutions, the investigation of other fault-tolerant topologies.

CRediT authorship contribution statement

Renato Bruni: Writing – review & editing, Writing – original draft, Methodology, Investigation, Formal analysis, Conceptualization. **Alberto Geri:** Validation, Supervision. **Marco Maccioni:** Writing – review & editing, Writing – original draft, Methodology, Investigation, Data curation, Conceptualization. **Ludovico Nati:** Writing – review & editing, Writing – original draft, Software, Methodology, Investigation, Data curation, Conceptualization.

Appendix

This Section describes reformulations based on cut-sets for the formulations (7)–(11) and (12)–(16) proposed in Section 3. The obtained constraints can be practically used to add another family of inequalities, in particular for formulation (12)–(16), which in our experiments appears to be the harder to solve.

When constraints (8) (or the equivalent constraints (13)) are enforced, then the following equation is satisfied, where S is as considered in (9):

$$\sum_{e\in E(S)} x_e + \frac{1}{2}\sum_{e\in\delta(S)} x_e = |S| \qquad \forall S \subseteq D \tag{A.1}$$

Proof. By Eq. (8) we know that the sum of the variables associated with the arcs incident to each demand node is equal to 2, even for a fractional solutions. Summing for each node $d \in S$, $S \subseteq D$ we are counting twice each arc in $E(S)$ and once each arc with only one endpoint in S, so we get:

$$\sum_{d\in S}\sum_{e\in\delta(d)} x_e = 2\sum_{e\in E(S)} x_e + \sum_{e\in\delta(S)} x_e = 2|S|.$$

Now we simply divide by 2 and we obtain (A.1).

Eq. (A.1) shows that $\sum_{e\in E(S)} x_e \le |S|-1$ if and only if $\sum_{e\in\delta(S)} x_e \ge 2$. Thus, if we replace (9) in formulation (7)–(11) by $\sum_{e\in\delta(S)} x_e \ge 2 \quad \forall S \subseteq D$, we obtain the following formulation based on cut-sets which is equivalent, in the sense that both define the same LP region.

$$\min \sum_{(i,j)\in A} c_{ij}\, x_{ij} \tag{A.2}$$

s.t.

$$\sum_{(i,j)\in\delta(k)} x_{ij} = 2 \qquad \forall k \in D \tag{A.3}$$

$$\sum_{e\in\delta(S)} x_e \ge 2 \qquad \forall S \subseteq D,\ |S| \ge 2 \tag{A.4}$$

$$\sum_{(i,j)\in\delta^-(k)} f_{ij} = d_k + \sum_{(i,j)\in\delta^+(k)} f_{ij} \qquad \forall k \in D \tag{A.5}$$

$$-(x_{ij}p_{ij})/2 \le f_{ij} \le (x_{ij}p_{ij})/2 \qquad \forall (i,j) \in A \tag{A.6}$$

$$x_{ij} \in \{0,1\} \qquad \forall (i,j) \in A$$

In order to derive now a formulation equivalent to (12)–(16) and based on cut-sets, recall that Eq. (14) spans either subsets composed of demand nodes only, or subsets containing demand nodes and exactly one root. For the subsets composed of demand nodes only, the equivalence between (14) and constraints based on cut-sets in the form of (A.4) can be proved as already explained above.

For a subset S with exactly one root $r \in R$, on the other hand, denote now by $S' = S \cap D$ (i.e., the set of demand nodes in S) and by $T = N \setminus (S)$ (i.e., the set of nodes outside of S). We can now rearrange Eq. (A.1) observing that $\delta(S') = \delta(S', r) \cup \delta(S', T)$ (we split the cut $\delta(S')$ in two parts: the arcs incident on r and those incident on T).

$$\sum_{e\in E(S)} x_e + \frac{1}{2}\left(\sum_{e\in\delta(S',T)} x_e - \sum_{e\in\delta(S',r)} x_e\right) = |S| - 1 \tag{A.7}$$

This equation shows that $\sum_{e\in E(S)} x_e \le |S| - 1$ if and only if

$$\sum_{e\in\delta(S',T)} x_e \ge \sum_{e\in\delta(S',r)} x_e. \tag{A.8}$$

This proves the equivalence between the constraints (14) on subsets S with exactly one root and constraints of type (A.8). Roughly speaking, constraint (A.8) imposes that the "amount" of x going from the set of demand node S' to the rest of the nodes T must be not smaller than the "amount" of x going from the same set of demand nodes S' to r (the only root in S). In terms of power lines, this can be interpreted as follows: there are no power lines serving the nodes S' and closing both extremes on the same root r if the number of lines serving the nodes S' and attached to r is not greater than the number of lines serving the same nodes S' and attached to nodes different from S. Thus, we have a formulation based on cut-sets equivalent to (12)–(16), splitting the case of subset S containing only demand nodes in (A.11) and subset S containing demand nodes and exactly one root in (A.12).

$$\min \sum_{(i,j)\in A} c_{ij}\, x_{ij} \tag{A.9}$$

s.t.

$$\sum_{(i,j)\in\delta(k)} x_{ij} = 2 \qquad \forall k \in D \tag{A.10}$$

$$\sum_{e\in\delta(S)} x_e \ge 2 \qquad \forall S \subseteq D,\ |S| \ge 2 \tag{A.11}$$

$$\sum_{e\in\delta(S,N-(S+r))} x_e - \sum_{e\in\delta(S,r)} x_e \ge 0 \qquad \forall S \subseteq D, r \in R \tag{A.12}$$

$$\sum_{(i,j)\in\delta^-(k)} f_{ij} = d_k + \sum_{(i,j)\in\delta^+(k)} f_{ij} \qquad \forall k \in D \tag{A.13}$$

$$-(x_{ij}p_{ij})/2 \le f_{ij} \le (x_{ij}p_{ij})/2 \qquad \forall (i,j) \in A \tag{A.14}$$

$$x_{ij} \in \{0,1\} \qquad \forall (i,j) \in A$$

Data availability

The data are available in Maccioni, M., Bruni, R., Nati, L., 2024. Optimal planning of power distribution networks with fault-tolerant configuration — dataset. https://doi.org/10.17632/8dp2mmf6t9.1.

References

Asensio, M., Meneses de Quevedo, P., Muñoz-Delgado, G., Contreras, J., 2018a. Joint distribution network and renewable energy expansion planning considering demand response and energy storage—Part I: Stochastic programming model. IEEE Trans. Smart Grid 9 (2), 655–666. http://dx.doi.org/10.1109/TSG.2016.2560339.

Asensio, M., Meneses de Quevedo, P., Muñoz-Delgado, G., Contreras, J., 2018b. Joint distribution network and renewable energy expansion planning considering demand response and energy storage—Part II: Numerical results. IEEE Trans. Smart Grid 9 (2), 667–675. http://dx.doi.org/10.1109/TSG.2016.2560341.

Avella, P., Villacci, D., Sforza, A., 2005. A steiner arborescence model for the feeder reconfiguration in electric distribution networks. European J. Oper. Res. 164 (2), 505–509. http://dx.doi.org/10.1016/j.ejor.2001.11.002.

Bosisio, A., Amaldi, E., Berizzi, A., Bovo, C., Fratti, S., 2015. A MILP approach to plan an electric urban distribution network with an H-shaped layout. In: 2015 IEEE Eindhoven PowerTech. IEEE, http://dx.doi.org/10.1109/PTC.2015.7232652.

Bosisio, A., Berizzi, A., Amaldi, E., Bovo, C., Sun, X.A., 2020. Optimal feeder routing in urban distribution networks planning with layout constraints and losses. J. Mod. Power Syst. Clean Energy 8 (5), 1005–1014. http://dx.doi.org/10.35833/MPCE.2019.000601.

Bosisio, A., Berizzi, A., Bovo, C., Amaldi, E., 2017. Urban distribution network planning with 2-step ladder topology considering joint nodes. In: 2017 IEEE Manchester PowerTech. IEEE, http://dx.doi.org/10.1109/PTC.2017.7980959.

Crainic, T.G., Gendreau, M., Gendron, B. (Eds.), 2021. Network Design with Applications To Transportation and Logistics, first ed. Springer.

Díaz-Dorado, E., Cidrás, J., Míguez, E., 2002. Application of evolutionary algorithms for the planning of urban distribution networks of medium voltage. IEEE Trans. Power Syst. 17 (3), 879–884. http://dx.doi.org/10.1109/TPWRS.2002.800975.

García, V.J., França, P.M., 2008. Multiobjective service restoration in electric distribution networks using a local search based heuristic. European J. Oper. Res. 189 (3), 694–705. http://dx.doi.org/10.1016/j.ejor.2006.07.048.

Glamocanin, V., Filipovic, V., 1993. Open loop distribution system design. IEEE Trans. Power Deliv. 8 (4), 1900–1906. http://dx.doi.org/10.1109/61.248300.

Gouin, V., Alvarez-Hérault, M.C., Raison, B., 2015. Optimal planning of urban distribution network considering its topology. In: 23rd International Conference on Electricity Distribution.

Gouin, V., Alvarez-Hérault, M.C., Raison, B., 2017. Innovative planning method for the construction of electrical distribution network master plans. Sustain. Energy Grids Netw. 10, 84–91. http://dx.doi.org/10.1016/j.segan.2017.03.004.

Gust, G., Schlüter, A., Feuerriegel, S., Úbeda, I., Lee, J.T., Neumann, D., 2024. Designing electricity distribution networks: The impact of demand coincidence. European J. Oper. Res. 315 (1), 271–288. http://dx.doi.org/10.1016/j.ejor.2023.11.029.

Hu, X., Ma, J., Zhang, R., Ma, D., Wang, Q., 2025. Ts-GSAN: A two-stage graphical spatiotemporal attention network fault localization method for distributed energy systems. IEEE Trans. Instrum. Meas. 74, 1–8. http://dx.doi.org/10.1109/TIM.2025.3548064.

Jabr, R.A., 2013. Polyhedral formulations and loop elimination constraints for distribution network expansion planning. IEEE Trans. Power Syst. 28 (2), 1888–1897. http://dx.doi.org/10.1109/TPWRS.2012.2230652.

Jooshaki, M., Abbaspour, A., Fotuhi-Firuzabad, M., Muñoz-Delgado, G., Contreras, J., Lehtonen, M., 2020. Linear formulations for topology-variable-based distribution system reliability assessment considering switching interruptions. IEEE Trans. Smart Grid 11 (5), 4032–4043. http://dx.doi.org/10.1109/TSG.2020.2991661.

Jooshaki, M., Abbaspour, A., Fotuhi-Firuzabad, M., Muñoz-Delgado, G., Contreras, J., Lehtonen, M., 2022. An enhanced MILP model for multistage reliability-constrained distribution network expansion planning. IEEE Trans. Power Syst. 37 (1), 118–131. http://dx.doi.org/10.1109/TPWRS.2021.3098065.

Lavorato, M., Franco, J.F., Rider, M.J., Romero, R., 2012. Imposing radiality constraints in distribution system optimization problems. IEEE Trans. Power Syst. 27 (1), 172–180. http://dx.doi.org/10.1109/TPWRS.2011.2161349.

Levitin, G., Mazal-Tov, S., Elmakis, D., 1995. Genetic algorithm for open-loop distribution system design. Electr. Power Syst. Res. 32 (2), 81–87. http://dx.doi.org/10.1016/0378-7796(94)00909-N.

Li, Z., Wu, W., Tai, X., Zhang, B., 2021. A reliability-constrained expansion planning model for mesh distribution networks. IEEE Trans. Power Syst. 36 (2), 948–960. http://dx.doi.org/10.1109/TPWRS.2020.3015061.

Li, Z., Wu, W., Zhang, B., Tai, X., 2020. Analytical reliability assessment method for complex distribution networks considering post-fault network reconfiguration. IEEE Trans. Power Syst. 35 (2), 1457–1467. http://dx.doi.org/10.1109/TPWRS.2019.2936543.

Ma, D., Hu, X., Zhang, H., Sun, Q., Xie, X., 2021. A hierarchical event detection method based on spectral theory of multidimensional matrix for power system. IEEE Trans. Syst. Man Cybern.: Syst. 51 (4), 2173–2186. http://dx.doi.org/10.1109/TSMC.2019.2931316.

Maccioni, M., Bruni, R., Nati, L., 2024. Optimal planning of power distribution networks with fault-tolerant configuration - Dataset [dataset]. In: Mendeley Data. http://dx.doi.org/10.17632/8dp2mmf6t9.1.

Muñoz-Delgado, G., Contreras, J., Arroyo, J.M., 2018a. Distribution network expansion planning with an explicit formulation for reliability assessment. IEEE Trans. Power Syst. 33 (3), 2583–2596. http://dx.doi.org/10.1109/TPWRS.2017.2764331.

Muñoz-Delgado, G., Contreras, J., Arroyo, J.M., 2018b. Reliability assessment for distribution optimization models: A non-simulation-based linear programming approach. IEEE Trans. Smart Grid 9 (4), 3048–3059. http://dx.doi.org/10.1109/TSG.2016.2624898.

Muñoz-Delgado, G., Contreras, J., Arroyo, J.M., 2018c. Distribution system expansion planning. In: Shahnia, F., Arefi, A., Ledwich, G. (Eds.), Electric Distribution Network Planning. Springer, pp. 1–40.

Nati, L., Bruni, R., Maccioni, M., Geri, A., 2025. Efficient handling of radiality constraints for large-scaled power distribution networks. Electr. Power Syst. Res. 241, 111278. http://dx.doi.org/10.1016/j.epsr.2024.111278.

Nemhauser, G., Wolsey, L.A., 1999. Integer and Combinatorial Optimization. Wiley.

Rastgou, A., 2024. Distribution network expansion planning: An updated review of current methods and new challenges. Renew. Sustain. Energy Rev. 189 (Pt B), 114062. http://dx.doi.org/10.1016/j.rser.2023.114062.

Tarjan, R.E., 1974. A note on finding the bridges of a graph. Inform. Process. Lett. 2 (6), 160–161. http://dx.doi.org/10.1016/0020-0190(74)90003-9.

Wang, Y., Xu, Y., Li, J., He, J., Wang, X., 2020. On the radiality constraints for distribution system restoration and reconfiguration problems. IEEE Trans. Power Syst. 35 (4), 3294–3296. http://dx.doi.org/10.1109/TPWRS.2020.2991356.

Wang, M., Yang, M., Fang, Z., Wang, M., Wu, Q., 2023. A practical feeder planning model for Urban distribution system. IEEE Trans. Power Syst. 38 (2), 1297–1308. http://dx.doi.org/10.1109/TPWRS.2022.3170933.

Wolsey, L.A., 2020. Integer Programming, second ed. Wiley.